



# Application and Development of Atomic Layer Deposition Techniques to Improve Thermo-optical Coatings for Spacecraft Thermal Control and Advanced Optical Instruments

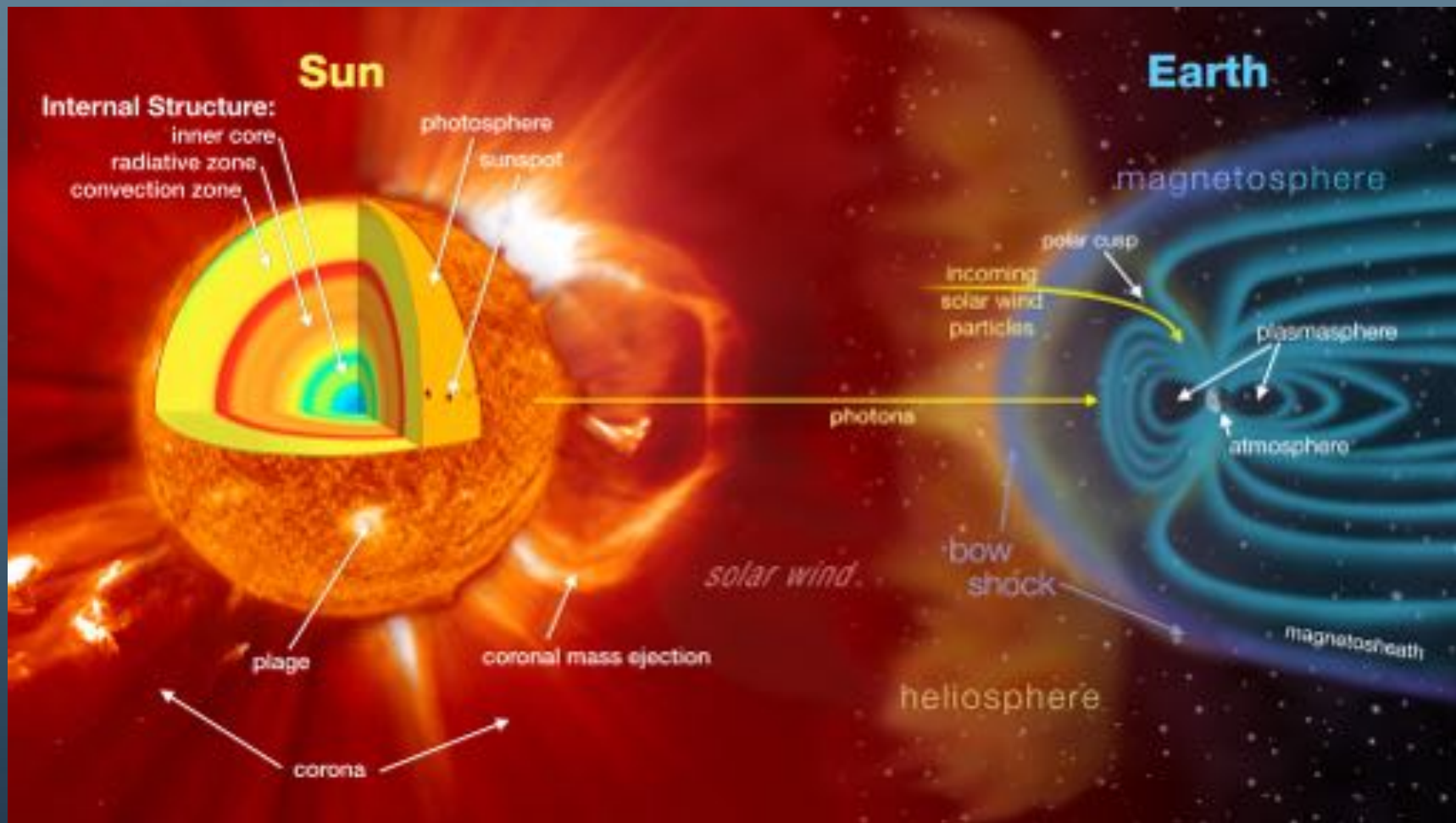
Dr. Vivek H. Dwivedi<sup>1</sup>,

Mark Hasegawa<sup>1</sup>, Raymond Adomaitis<sup>2</sup>, Hossein Salami<sup>2</sup>

<sup>1</sup>*NASA Goddard Space Flight Center Greenbelt, MD. 20771*

<sup>2</sup>*University of Maryland College Park, Department of Chemical and Biomolecular Engineering College Park, MD. 20742*

# Sun – Earth Connection

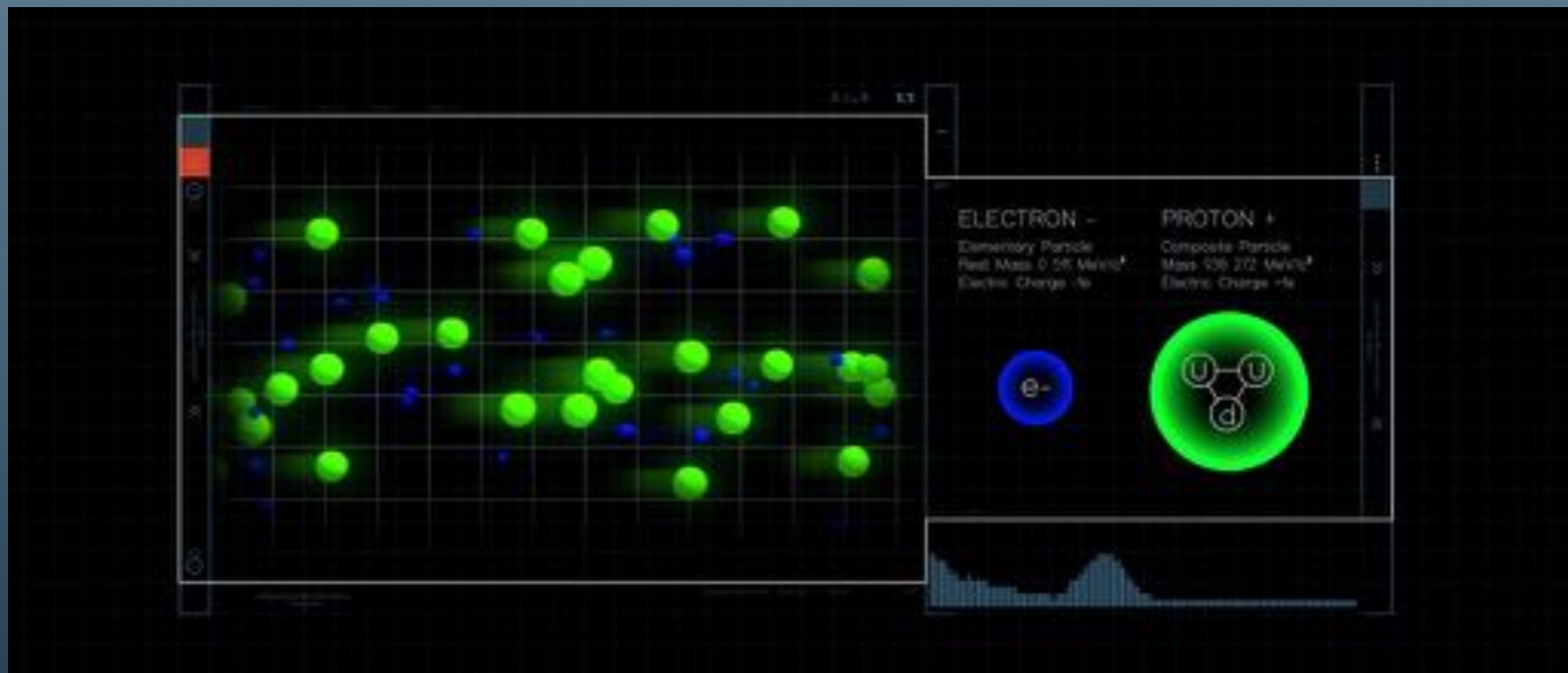




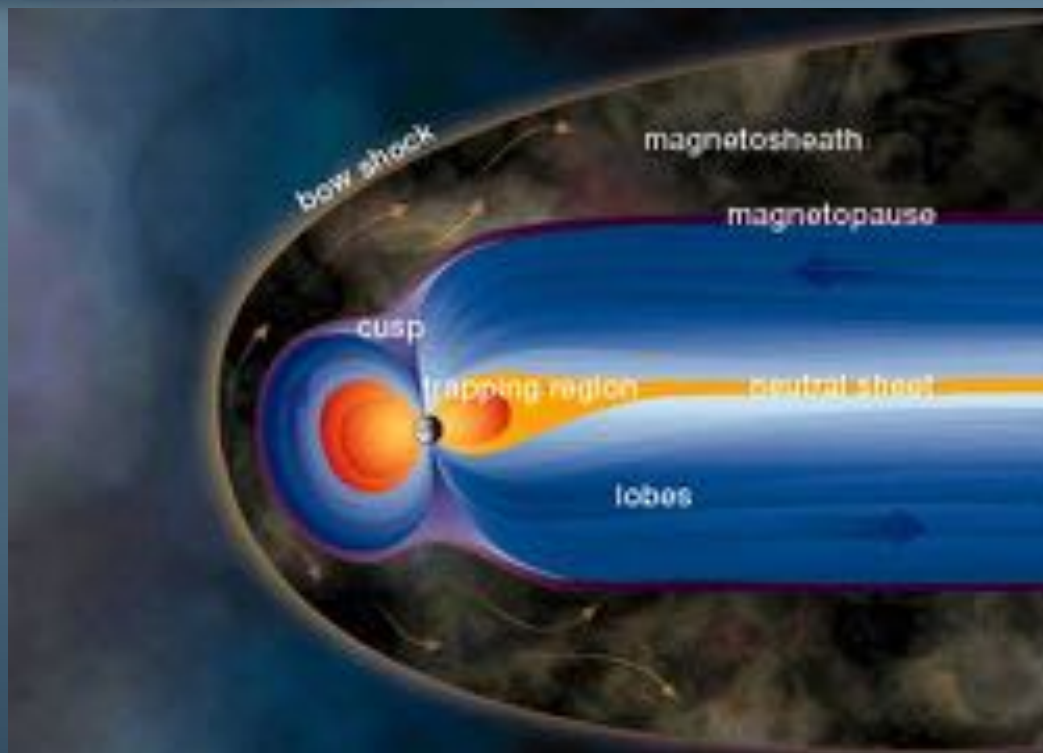
# Sun – Earth Connection



# Sun – Earth Connection

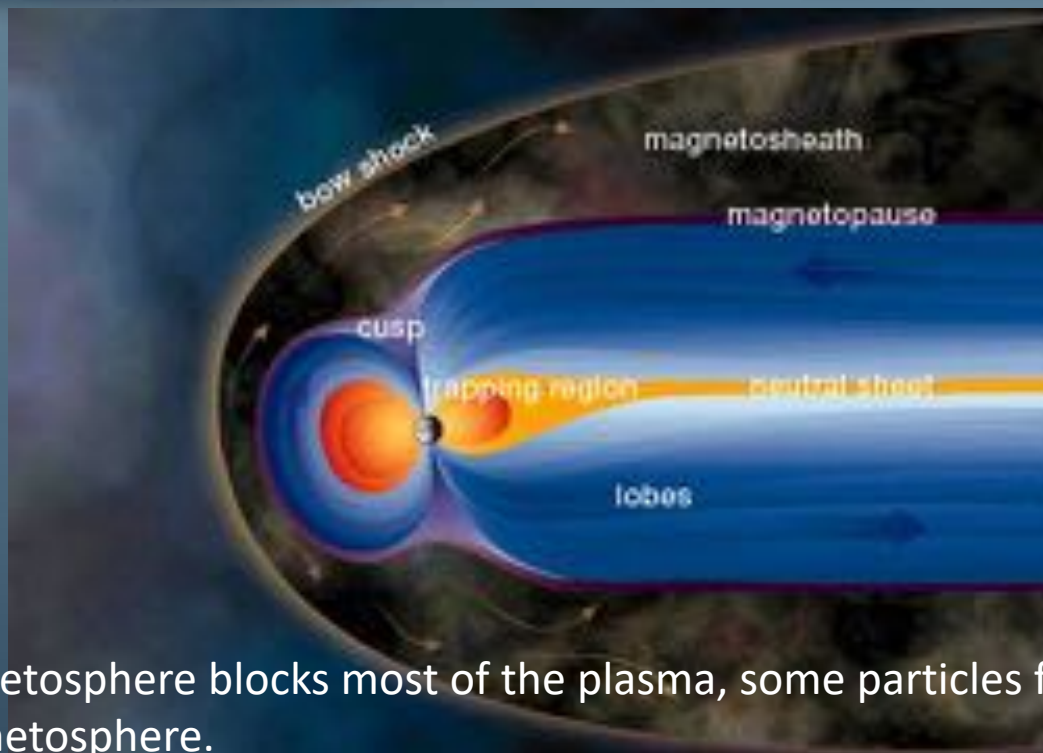


# Sun – Earth Connection



The picture above illustrates the magnetosphere and labels several of its key components

# Sun – Earth Connection

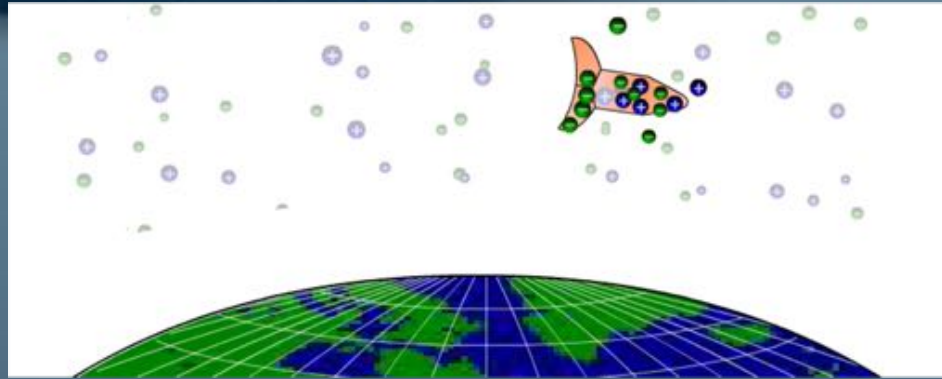


Although the magnetosphere blocks most of the plasma, some particles from the solar wind can enter the magnetosphere.

The particles that enter from the magnetotail travel toward the Earth and create an aurora.

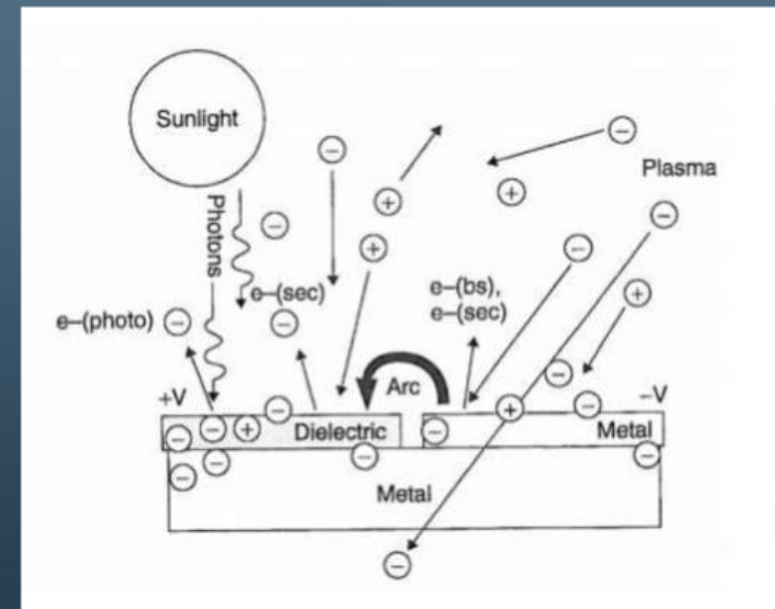
Trapping Region: the part of the magnetosphere that traps electrically charged particles (electrons, protons, and heavier atomic ions) or radiation; also known as radiation belt

# Spacecraft Charging



Surface charging occurs from low-energy plasma and photoelectric currents.

During the eclipse (while in the shadow of the earth) phase of an orbit the spacecraft may negatively charge to tens of kilovolts and once the satellite emerges into sunlight a photoelectron emission may occur resulting in a potential discharge.



Garrett, H. B., Whittlesey, A. C.; GUIDE TO MITIGATING SPACECRAFT CHARGING EF



# Problem

Spacecraft charging is the condition that occurs when a spacecraft accumulates excess electrons or ions. For a conducting spacecraft, the excess charges are on the surface. The term spacecraft surface charging (absolute charging) is used to clearly denote charging on the spacecraft surface as opposed to other charge distributions such as the voltage differences between electrically isolated parts of the spacecraft (differential charging).

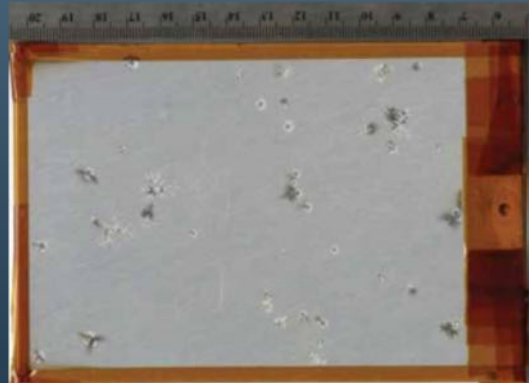
**HAZARD**

If a charge builds up that is too big for the spacecraft's material to hold, discharge arcs, which are essentially strong electrical currents, will occur.

And depending on where those arcs go, they can damage electronic components, destroy sensors, or damage important materials such as thermal control coatings.



ESA EURECA satellite solar array sustained arc damage.Credits: ESA



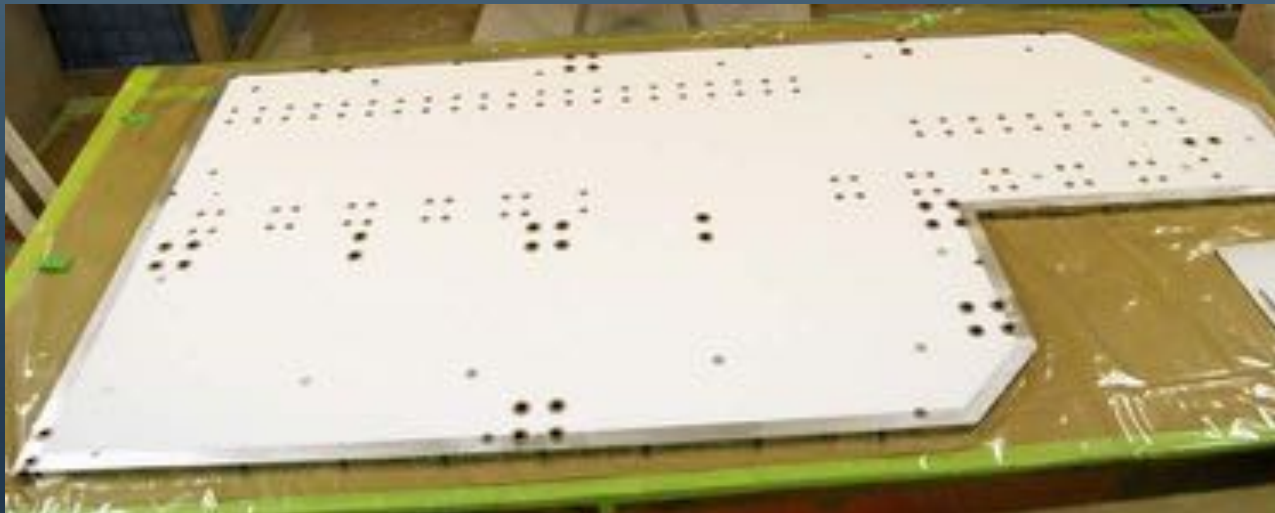
Arc damage in laboratory tests of the chromic acid anodized thermal control coating covering ISS orbital debris shields.Credits: NASA/T. Schneider

# Radiator



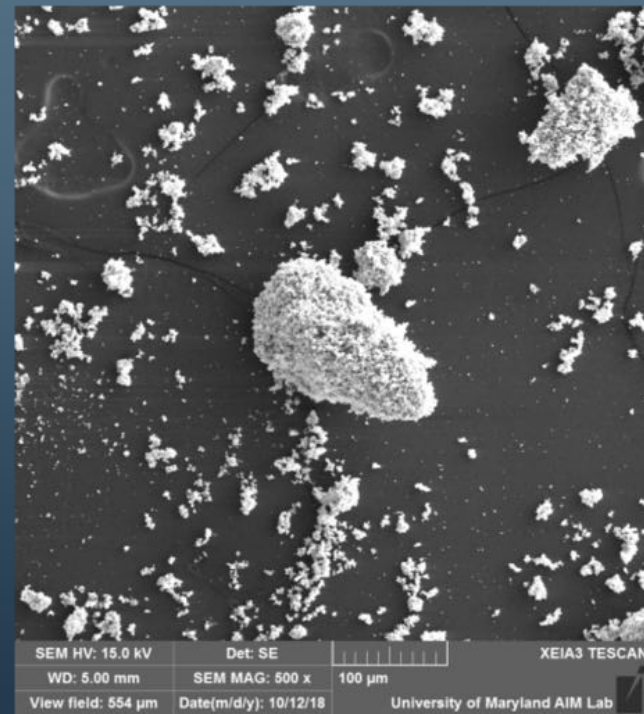
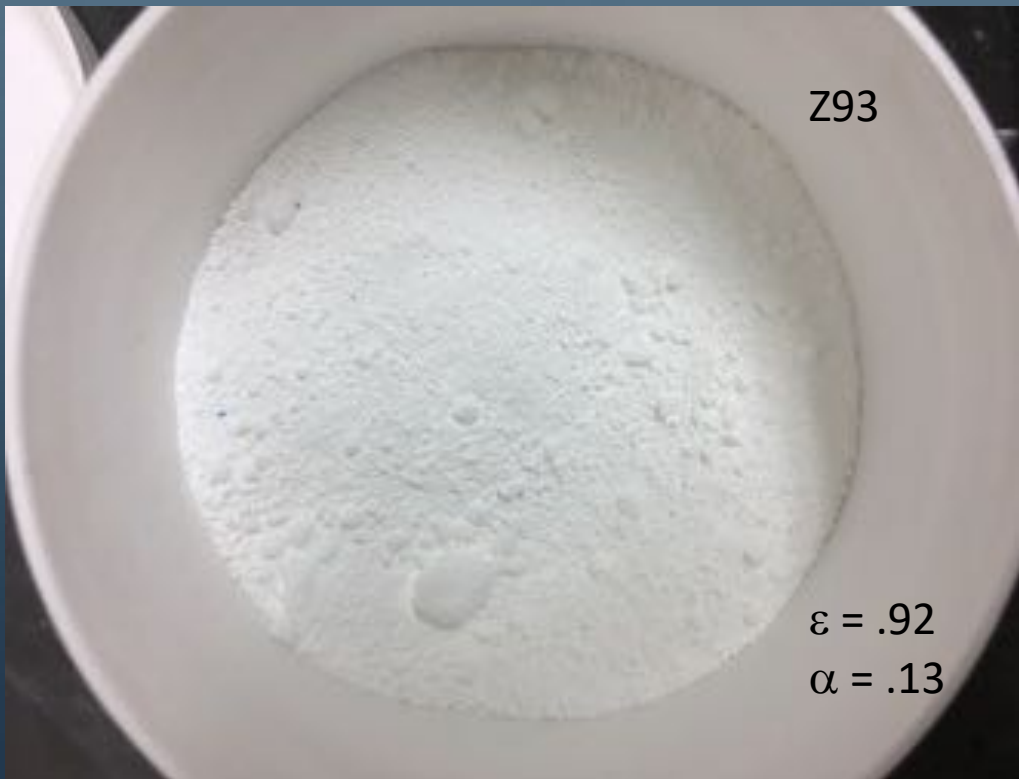
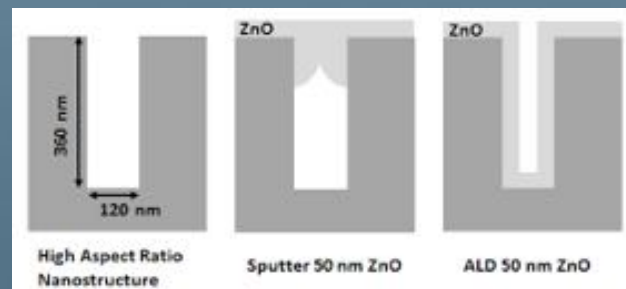
A dedicated structure whose purpose is the rejection of waste heat to deep space

- Coated with high emissivity coating to maximize heat rejection potential
- May be coated with high or low solar absorptivity coating depending on view to solar sources
- If not existing structure, then supports are needed
- **Coatings** – films, tapes, paints, etc. applied to surfaces to obtain the desired thermo-optical properties for thermal control
  - Thermo-optical properties are intrinsic to the material itself (e.g. white paint, black paint, Kapton, etc)
    - $\alpha$  – Solar Absorptivity – percentage of sun energy (Direct Solar, Albedo [e.g. reflected solar]) absorbed
    - $\varepsilon$  – IR Emissivity – percentage of planet energy (Planetshine) absorbed
      - *Also a measure of emissive capability of a surface to reject heat via IR radiation*
      - Because the (electrically) insulating pigment can become differentially charged in LEO or GEO orbits a mitigation technique is needed to “bleed” it off

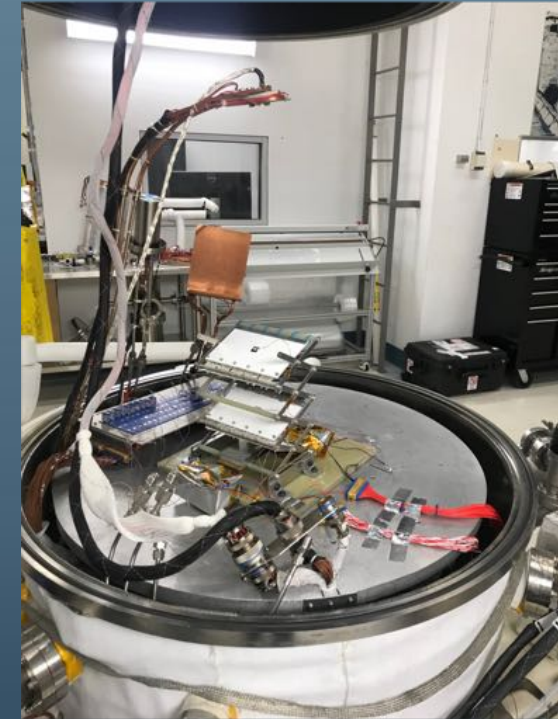
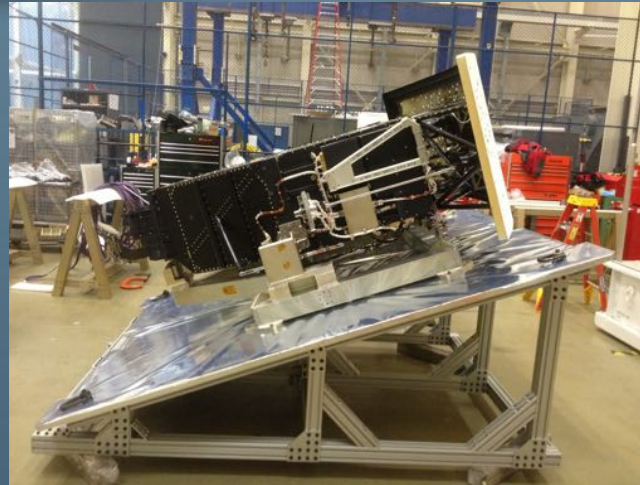


*Radiator with White Paint Coating*

# Background



# Radiator - Vary in Size



Origami Inspired



The space station's radiator system, which is a critical component of the active system, consists of seven panels (each about 6 by 12 feet)



Wide Field Planetary Camera 2 (WFPC2) that was installed on the Hubble Space Telescope in December 1993, and removed during the last servicing mission in 2009



# Motivation

- Most white pigments do not dissipate electrical charge without a dopant or additive
- Two most commonly used dissipative thermal coatings (Z93C55 and AZ2000) rely on indium hydroxide or tin oxide as charge dissipative additives utilizing sol gel wet chemistry
- ITO formed locally on a macroscopic scale due to seeding and ITO crystal formation on the boundaries of the pigment grains. Thickness and dispersion throughout the coating are difficult to control.

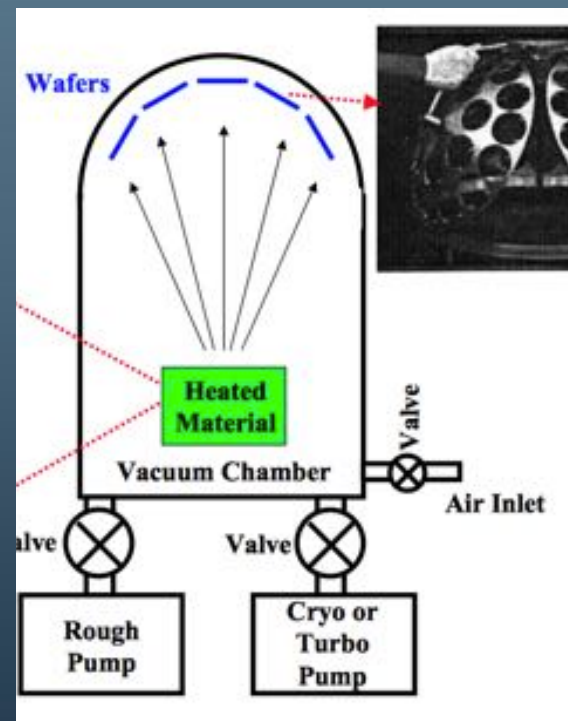
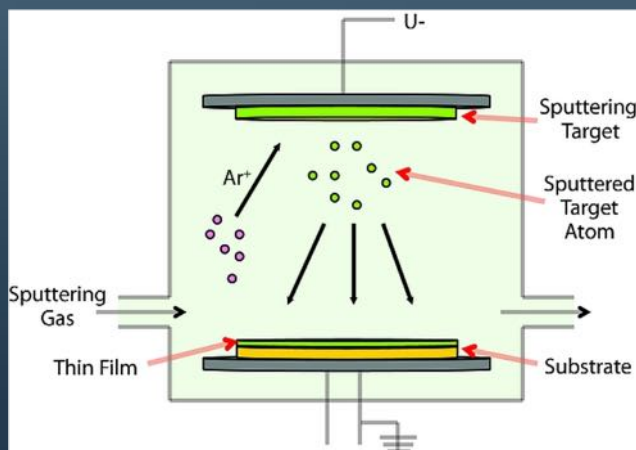
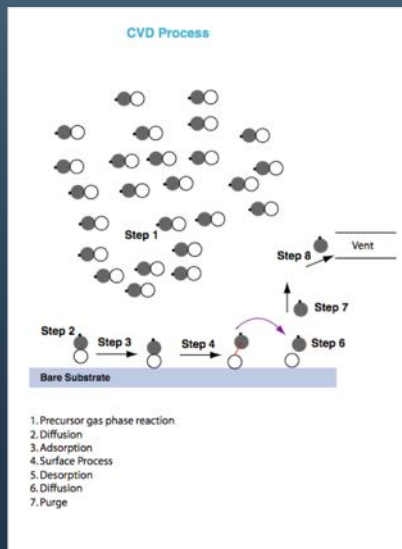
Instead of postprocessing the dissipative coating can we preprocess the dissipative coating before binding directly on the pigment itself?

# What is a Thin Film?

**Thin film:** thickness typically  $<1000\text{nm}$ .

**Special properties of thin films:** different from bulk materials, it may be –

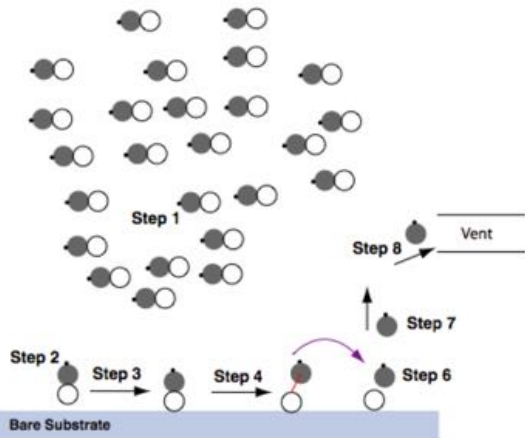
- Not fully dense
- Under stress
- Different defect structures from bulk
- Quasi - two dimensional (very thin films)
- Strongly influenced by surface and interface effects



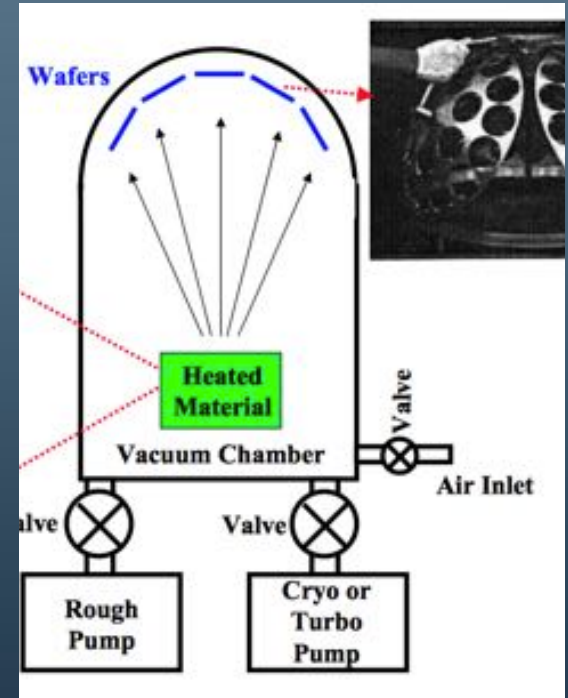
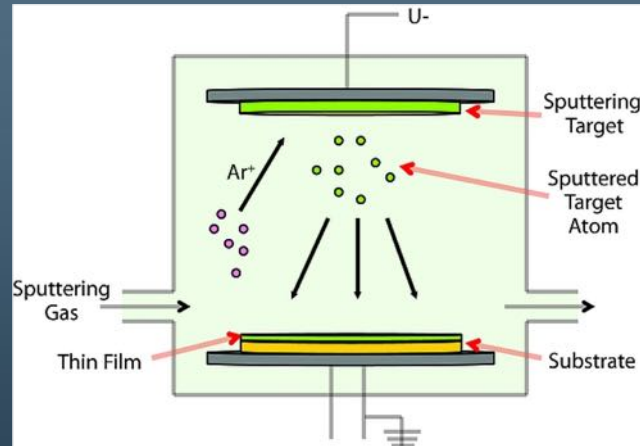
# Other Deposition Techniques



CVD Process



1. Precursor gas phase reaction
2. Diffusion
3. Adsorption
4. Surface Process
5. Desorption
6. Diffusion
7. Purge

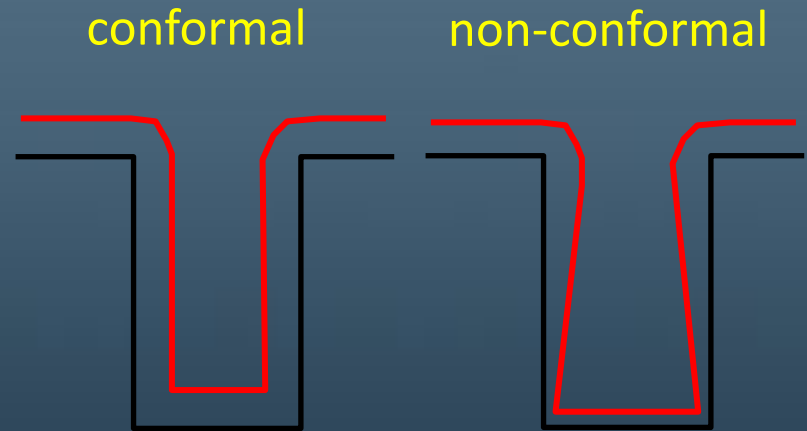
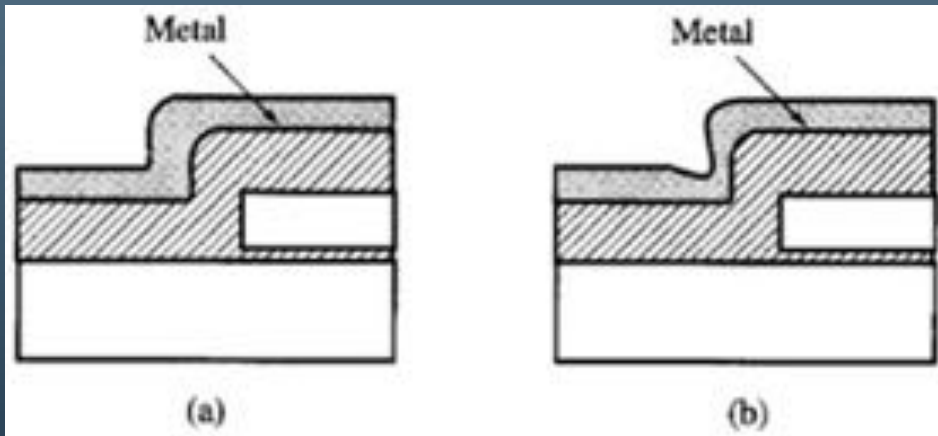


# Common Denominator



- Deposition only occurs on substrates that “see” the target.
- Plasma process can damage the substrate
- Poor thickness control
- Poor Step Control
- High Pressure High Temperature Environment

## Step Coverage Example



Step coverage of metal over non-planar topography.

(a) Conformal step coverage, with constant thickness on horizontal and vertical surfaces.

(b) Poor step coverage, here thinner for vertical surfaces.

# Atomic Layer Deposition



Atomic  
Layer  
Deposition



A thin film “nanomanufacturing” tool that allows for the conformal coating of materials on a myriad of surfaces with precise atomic thickness control.

Based on:

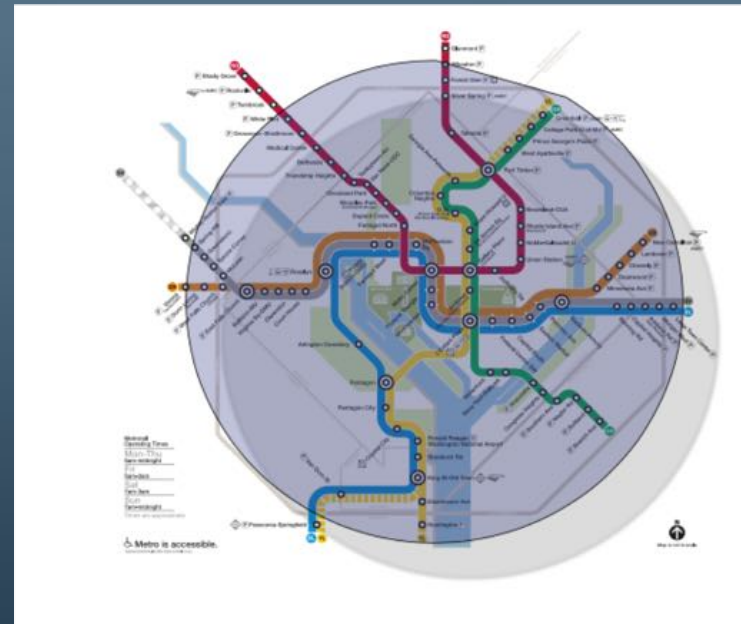
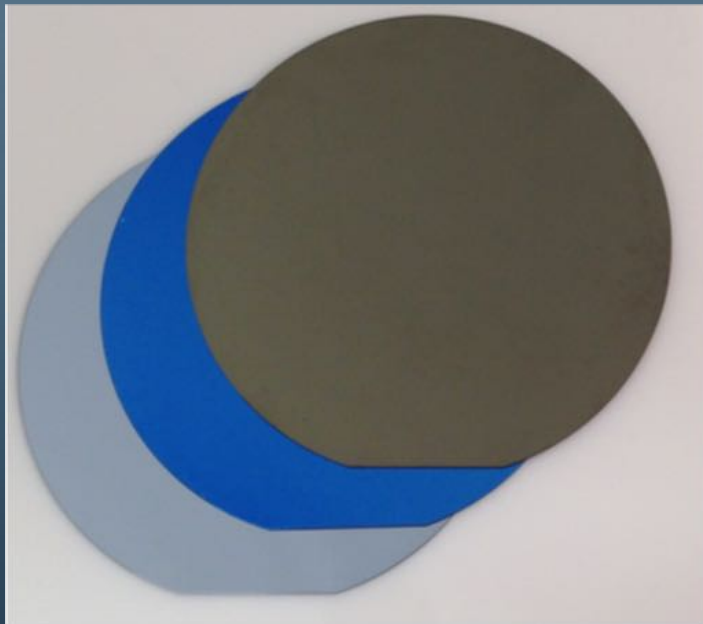
- Paired gas surface reaction chemistries
- Benign non-destructive temperature and pressure environment
  - Room temperature -> 250 °C (even lower around 45 °C)
  - Vacuum

# ALD

Precursor A + Precursor B  $\rightarrow$  Solid film + Gas by-products

Cyclic operation: A  $\rightarrow$  purge  $\rightarrow$  B  $\rightarrow$  purge  $\rightarrow$  A  $\rightarrow$  purge  $\rightarrow$  ...

Atomic-level thickness control ...

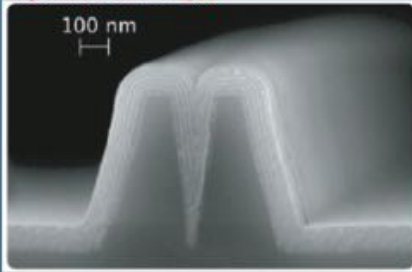


... equivalent to a 60  $\mu\text{m}$  layer over a city-sized wafer



# ALD Advantageous Property

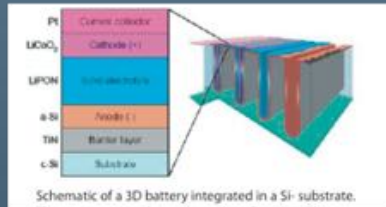
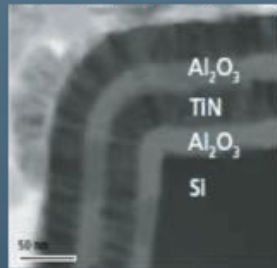
Artificial trench filled with an ALD nanolaminate  
Image courtesy of Austin University [20]



## Epitaxial Growth

Multilayer consisting of:  
Al<sub>2</sub>O<sub>3</sub> - 25 nm  
TiN - 20 nm  
Al<sub>2</sub>O<sub>3</sub> - 25 nm

Dr. Fred Roseboom, NXP Semiconductor Research and  
Dr. Edwin Kozak, University of Technology, Eindhoven



Schematic of a 3D battery integrated in a Si-substrate.  
The cross-section shows the various functional layers  
in the battery stack as well as the candidate materials.

Kozak, E.C.M. et al., *IEEE Trans.*, 26 (2009) pp. 133-144

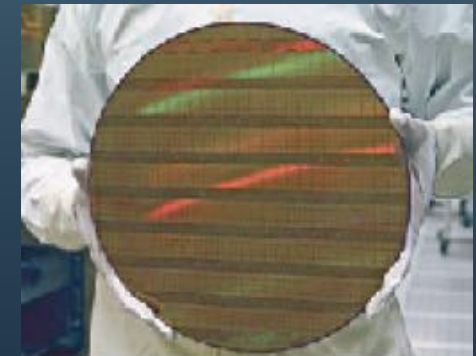
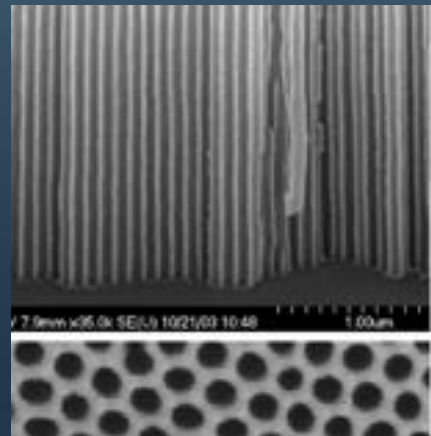
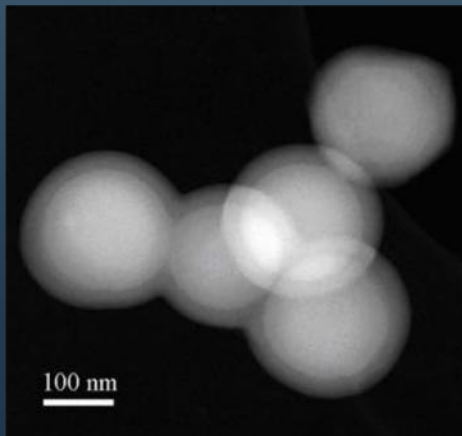
## Batch Process



Coating Silver with Aluminum Oxide  
<http://www.glassonweb.com>



## Substrate Independence



Goddard  
Space Flight Center

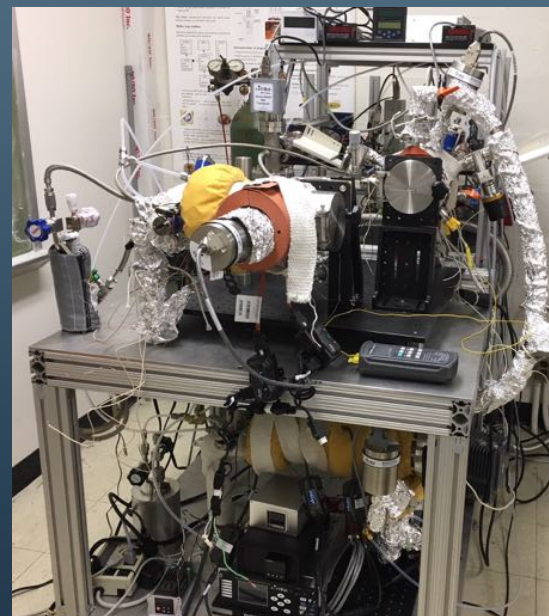
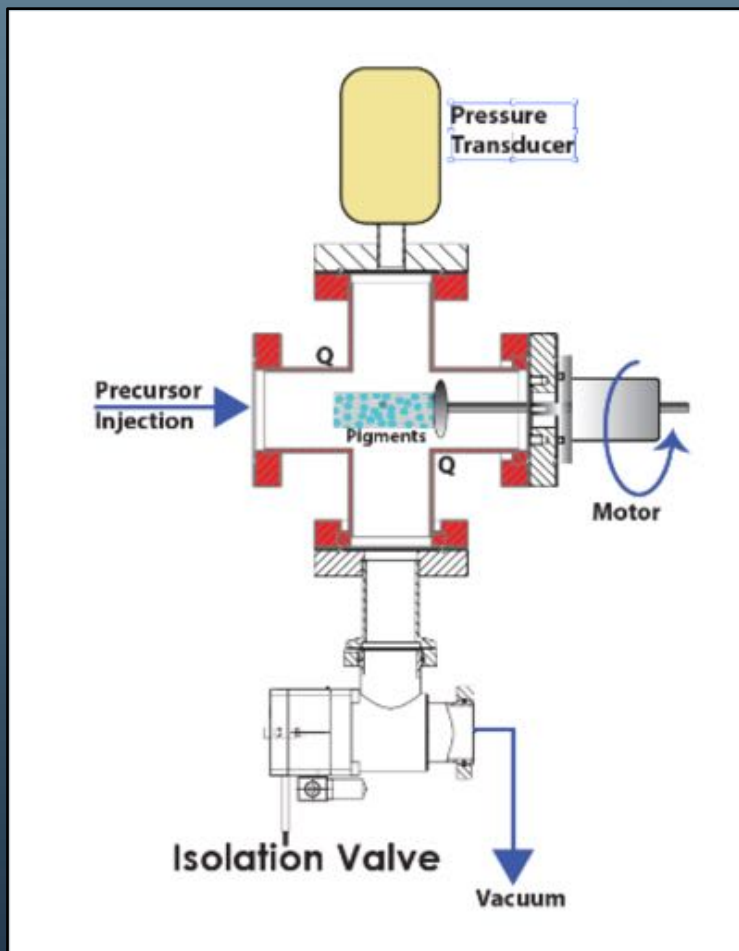


# ALD Material Systems

<p>O: Oxide      C: Carbide N: Nitride      F: Fluoride M: Metal      D: Dopant P: Phosphide/Arsenide S: Sulphide/Selenide/Telluride</p> <p><input type="checkbox"/> Oxide of this element has been deposited by the ALD community <input checked="" type="checkbox"/> Recipe for this material is available from CNT staff or customer base</p>																			
H 1																	He 2		
<input checked="" type="checkbox"/> Li 3	Be 4													<input checked="" type="checkbox"/> B 5	C 6	N 7	O 8	F 9	Ne 10
Na 11	<input checked="" type="checkbox"/> Mg 12													<input checked="" type="checkbox"/> Al 13	<input checked="" type="checkbox"/> Si 14	P 15	S 16	Cl 17	Ar 18
K 19	<input checked="" type="checkbox"/> Ca 20	<input checked="" type="checkbox"/> Sc 21	<input checked="" type="checkbox"/> Ti 22	<input checked="" type="checkbox"/> V 23	<input checked="" type="checkbox"/> Cr 24	<input checked="" type="checkbox"/> Mn 25	<input checked="" type="checkbox"/> Fe 26	<input checked="" type="checkbox"/> Co 27	<input checked="" type="checkbox"/> Ni 28	<input checked="" type="checkbox"/> Cu 29	<input checked="" type="checkbox"/> Zn 30	<input checked="" type="checkbox"/> Ga 31	<input checked="" type="checkbox"/> Ge 32	As 33	Se 34	Br 35	Kr 36		
Rb 37	<input checked="" type="checkbox"/> Sr 38	<input checked="" type="checkbox"/> Y 39	<input checked="" type="checkbox"/> Zr 40	<input checked="" type="checkbox"/> Nb 41	<input checked="" type="checkbox"/> Mo 42	Tc 43	<input checked="" type="checkbox"/> Ru 44	<input checked="" type="checkbox"/> Rh 45	<input checked="" type="checkbox"/> Pd 46	<input checked="" type="checkbox"/> Ag 47	<input checked="" type="checkbox"/> Cd 48	<input checked="" type="checkbox"/> In 49	<input checked="" type="checkbox"/> Sn 50	<input checked="" type="checkbox"/> Sb 51	Te 52	I 53	Xe 54		
Cs 55	<input checked="" type="checkbox"/> Ba 56	<input checked="" type="checkbox"/> La 57	<input checked="" type="checkbox"/> Hf 72	<input checked="" type="checkbox"/> Ta 73	<input checked="" type="checkbox"/> W 74	Re 75	<input checked="" type="checkbox"/> Os 76	<input checked="" type="checkbox"/> Ir 77	<input checked="" type="checkbox"/> Pt 78	<input checked="" type="checkbox"/> Au 79	<input checked="" type="checkbox"/> Hg 80	<input checked="" type="checkbox"/> Tl 81	<input checked="" type="checkbox"/> Pb 82	Bi 83	Po 84	At 85	Rn 86		
Fr 87	Ra 88	Ac 89	Rf 104	Db 105	Sg 106	Bh 107	Hs 108	Mt 109											
<p><input checked="" type="checkbox"/> Ce 58    <input checked="" type="checkbox"/> Pr 59    <input checked="" type="checkbox"/> Nd 60    <input checked="" type="checkbox"/> Pm 61    <input checked="" type="checkbox"/> Sm 62    <input checked="" type="checkbox"/> Eu 63    <input checked="" type="checkbox"/> Gd 64    <input checked="" type="checkbox"/> Tb 65    <input checked="" type="checkbox"/> Dy 66    <input checked="" type="checkbox"/> Ho 67    <input checked="" type="checkbox"/> Er 68    <input checked="" type="checkbox"/> Tm 69    <input checked="" type="checkbox"/> Yb 70    <input checked="" type="checkbox"/> Lu 71</p>																			
<p><input checked="" type="checkbox"/> Th 90    <input checked="" type="checkbox"/> Pa 91    <input checked="" type="checkbox"/> U 92    <input checked="" type="checkbox"/> Np 93    <input checked="" type="checkbox"/> Pu 94    <input checked="" type="checkbox"/> Am 95    <input checked="" type="checkbox"/> Cm 96    <input checked="" type="checkbox"/> Bk 97    <input checked="" type="checkbox"/> Cf 98    <input checked="" type="checkbox"/> Es 99    <input checked="" type="checkbox"/> Fm 100    <input checked="" type="checkbox"/> Md 101    <input checked="" type="checkbox"/> No 102    <input checked="" type="checkbox"/> Lr 103    <input checked="" type="checkbox"/> 4 104    <input checked="" type="checkbox"/> 4</p>																			

- Gordon, Roy (2008). Atomic Layer Deposition (ALD): An Enable for Nanoscience and Nanotechnology. PowerPoint lecture presented at Harvard University, Cambridge, MA.
- Elam, Jeffrey (2007). ALD Thin Film Materials. Argonne National Laboratory

# ALD For Radiators - Pigments



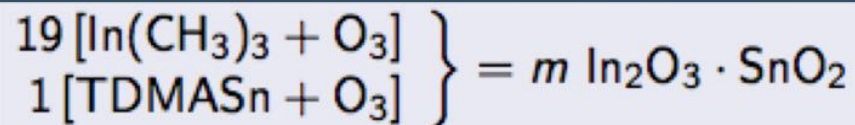


# In<sub>2</sub>O<sub>3</sub> and SnO<sub>2</sub> Chemistries

ALD of multi-material systems such as ITO requires that the films, in this instance metal oxides with ozone as the common oxidizer, have a deposition window that corresponds to an ALD growth window common to each precursor system.



For “standard 5%” Sn doped indium oxide we apply a super cycle





# Experimental Procedures

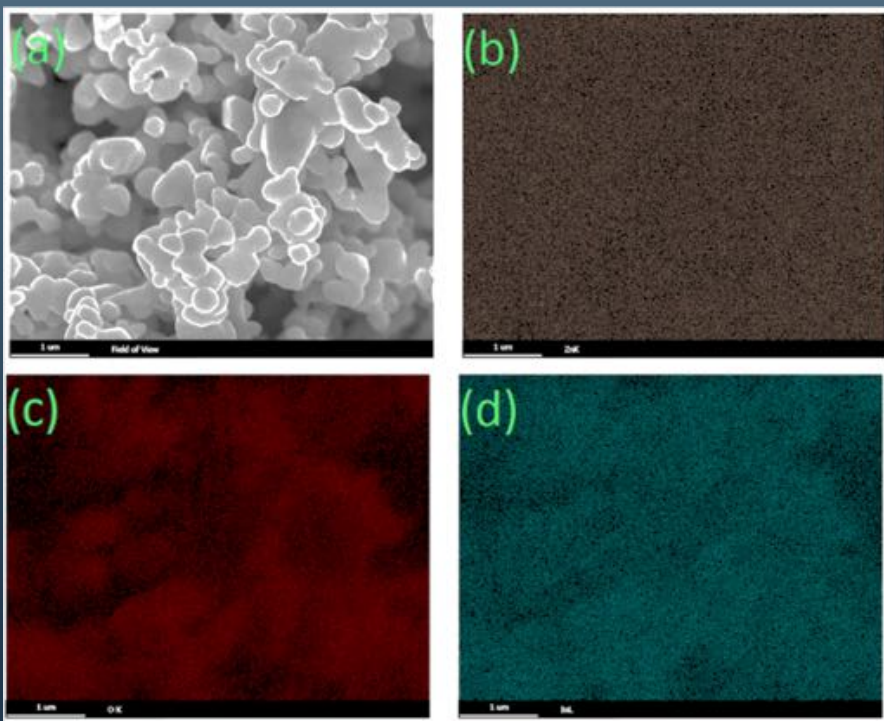
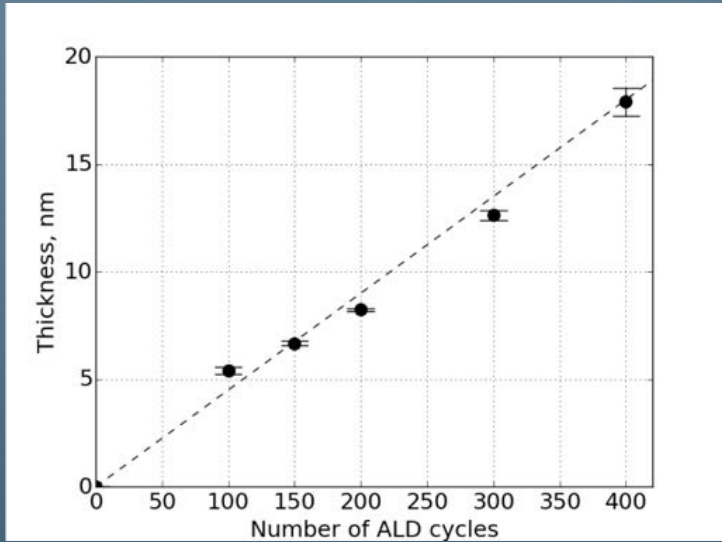
- The first set of experiments were conducted on flat substrates for the ALD of  $\text{In}_2\text{O}_3$  and ITO, the films were deposited on a variety of substrates including n-type Si(100) wafers for thickness measurements and glass microscope slides for sheet resistivity determination.
- The  $\text{In}_2\text{O}_3$  ALD on the particle substrates was applied to Z93P pigments provided by Alion Science and Technology; these particles had a mean size of 2 microns.
- Thickness and conformity of the ALD films on the Si wafers of  $\text{In}_2\text{O}_3$  and ITO were measured using a J.A. Woollam M-2000D Spectroscopic Ellipsometer. The sheet resistivity of the ALD films on the microscope glass substrates was measured using a Lucas Signatone S-302 four-point probe
- The bulk resistivity of the ALD deposited pigment system is measured in air after the formation of a pellet of 1 in. diameter and a thickness of approximately .5 in. The pigment is compressed lightly by hand and held in place by a 3D printed electrically insulating hollow nylon/Teflon annulus spacer held on an aluminum plate. Resistivity was measured in air and vacuum.

# Results

The growth Vs. the number of ALD cycles confirms a self-limiting gpc of **0.46 Å/cycle** for indium oxide.

A saturated growth was observed to result in gpc of **0.55 Å/cycle** independent of the process temperature.

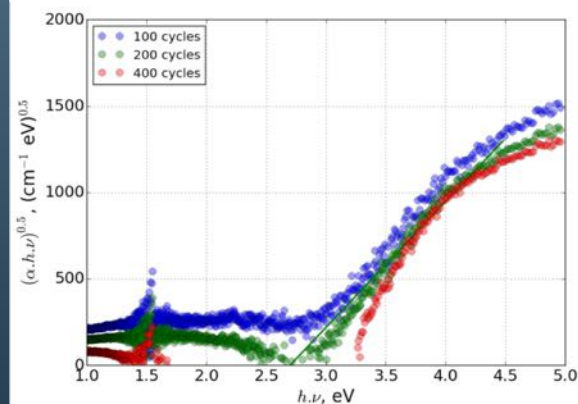
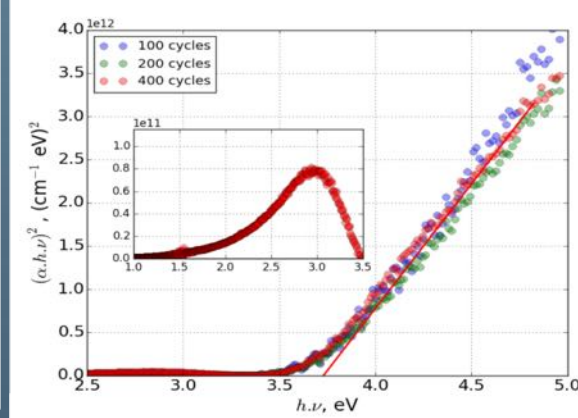
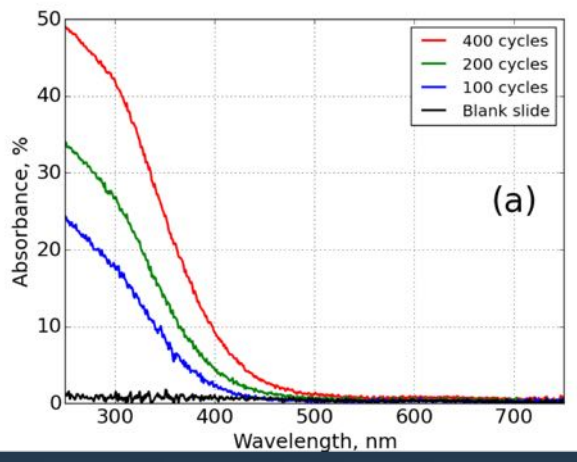
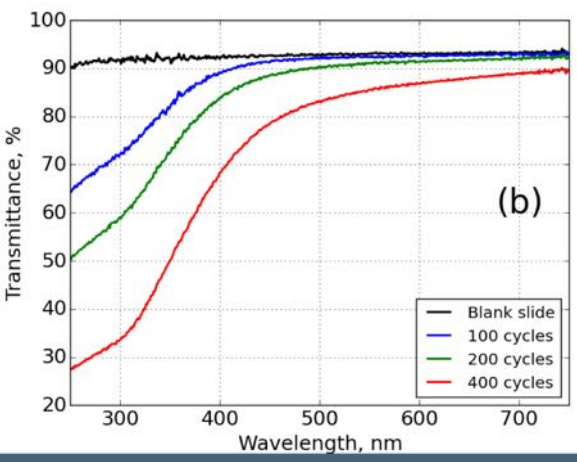
At 413K small crystal grains are formed 20nm in size. This is consistent with the onset of **crystallization** reported for similar system.



EDS scan of coated Z93 particles deposited with 600 ALD cycles at 135 °C in a regular flow-type ALD process. Image of the mapping area (a), Scan for Zn (b), O (c), and In (d). The black background is the carbon tape used for fixing the particles.



# Results



IO film deposited with 100 cycles shows about 90% transparency.

Tauc's procedure can be used to estimate the film band gap.  
 $n = 1/2$  for direct transitions  
 $n = 2$  for indirect transitions

$$\alpha = \frac{1}{d} \times \ln \left[ \frac{(1 - R)^2}{T} \right]$$

$$\alpha h\nu = A(h\nu - E_{g,opt})^n$$

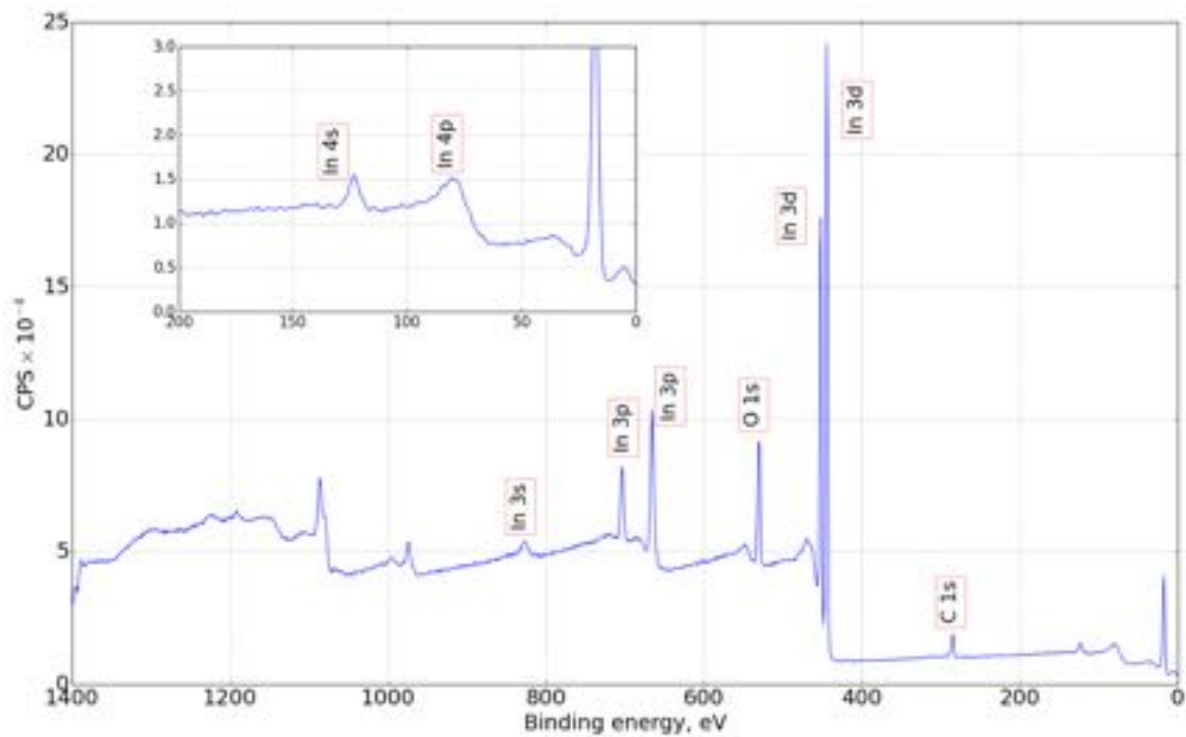
Direct band gap of 3.7 eV and indirect band gap of 2.6 eV can be estimated.

# Results

XPS analysis confirms the deposition of **indium oxide**.

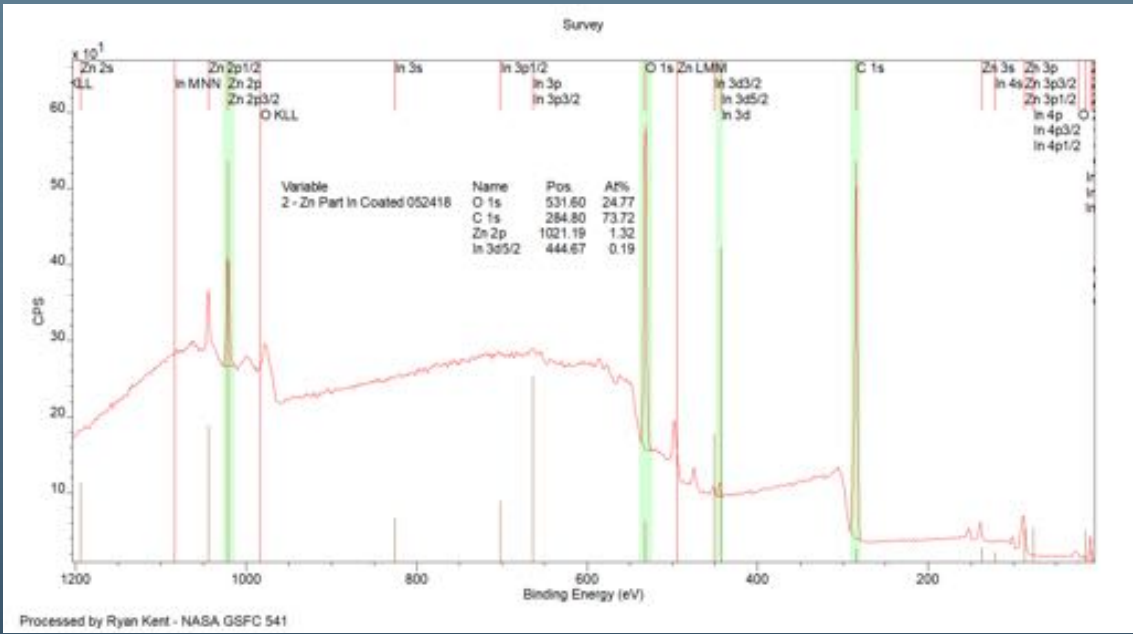
O/In < 1.5 ratio confirms a **n-type**

	140 (C)	190 (C)
<b>C</b>	26	16
<b>O</b>	44	48
<b>In</b>	30	36
<b>O/In</b>	1.44	1.33





# Results



Processed by Ryan Kent - NASA GSFC 541

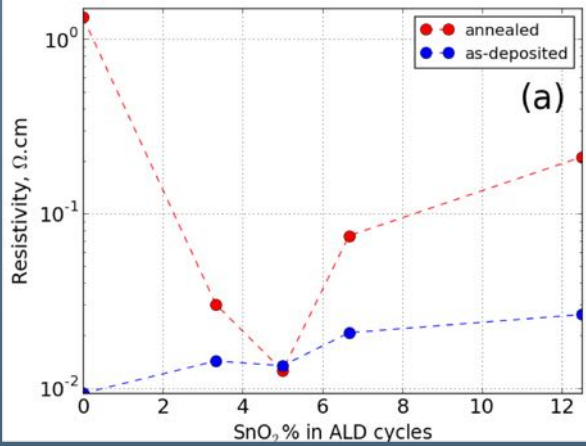
Spectrum Label	Zinc Oxide Particles	Indium Oxide Coated
C	57.73	73.72
O	33.23	24.76
Zn	9.04	1.28
In	-	0.23

## XPS of Particle Composition





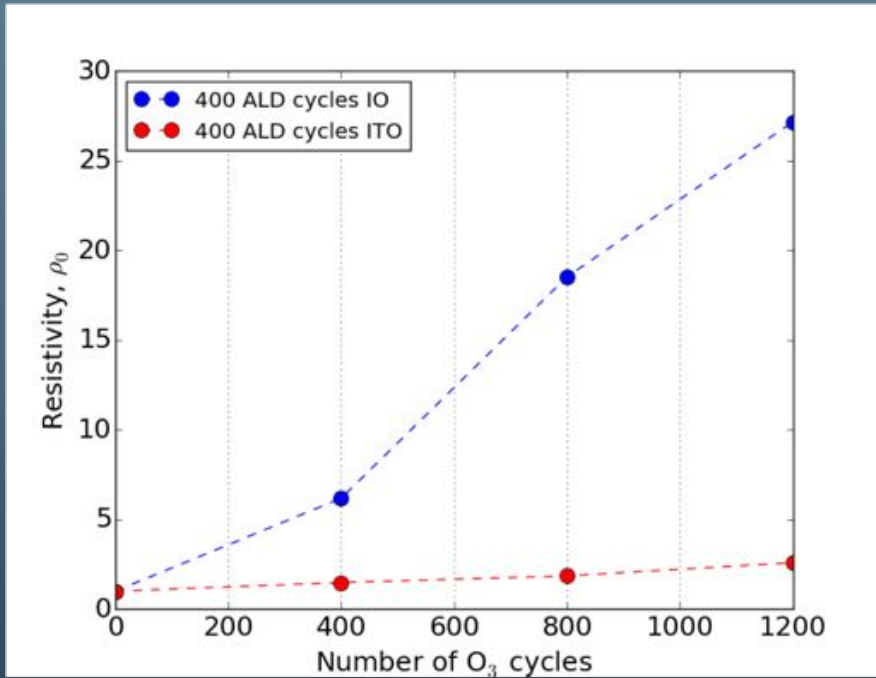
# Indium Tin Oxide



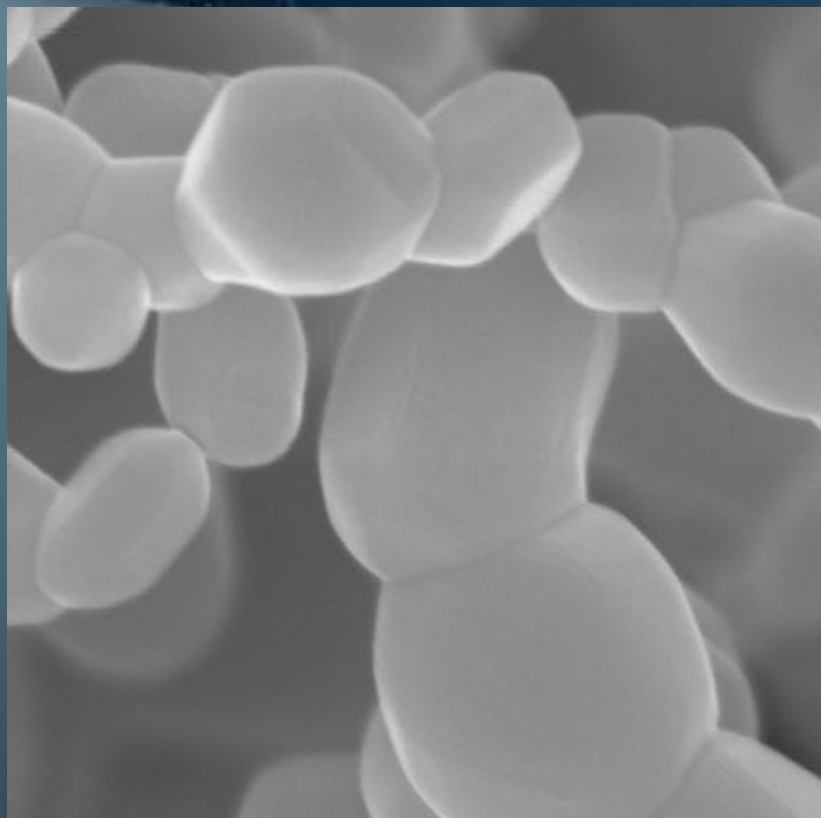
Deposited at 373K  
Annealed at 723K

Experimental data reported in the literature for IO film resistivity are **highly variable**.

**Optimally doped ITO** sample maintains its resistivity against ozone.

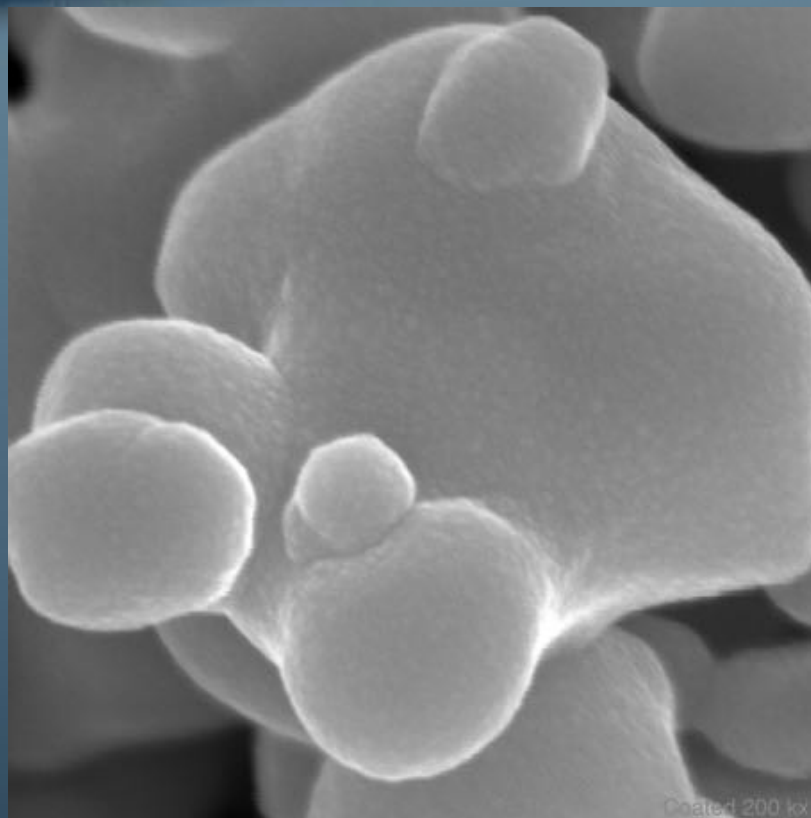


# Results



SEM HV: 15.0 kV	Det: In-Beam SE		XEIA3 TESCAN
WD: 4.93 mm	SEM MAG: 200 kx	200 nm	Uncoated 200 kx
View field: 1.38 $\mu$ m	Date(m/d/y): 10/12/18	University of Maryland AIM Lab	

**Uncoated Pigment**

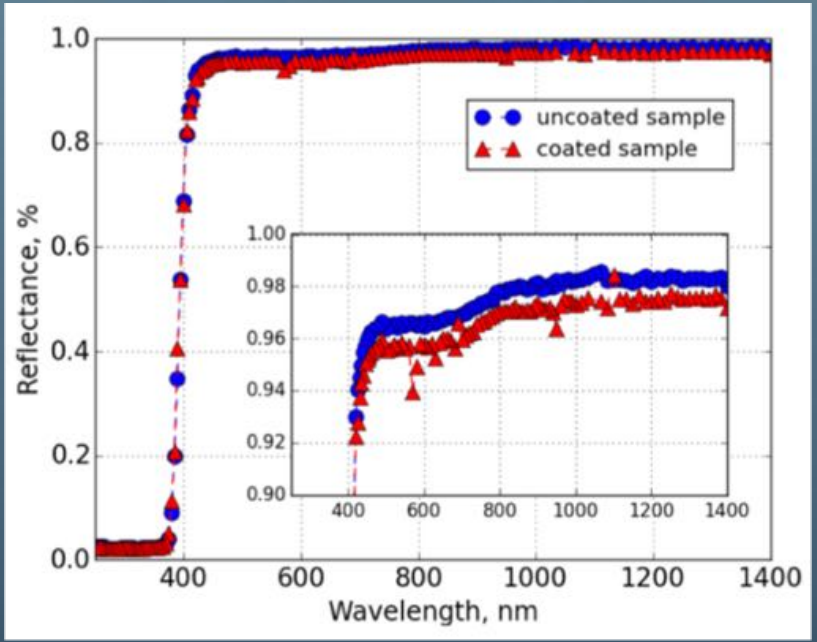


SEM HV: 15.0 kV	Det: In-Beam SE		XEIA3 TESCAN
WD: 5.00 mm	SEM MAG: 200 kx	200 nm	Coated 200 kx
View field: 1.38 $\mu$ m	Date(m/d/y): 10/12/18	University of Maryland AIM Lab	

**Coated Pigment**



# Results



Reflectance measurements were taken on lightly compressed pellets of the untreated and indium oxide treated Z93P pigment and show approximately one percent reflectance differences across the solar spectrum

	BOL (Cold Case)	
	Absorptivity ( $\alpha$ )	Emissivity ( $\epsilon$ )
Z93	0.13	0.92
Coated Z93	0.14	0.92



# Results

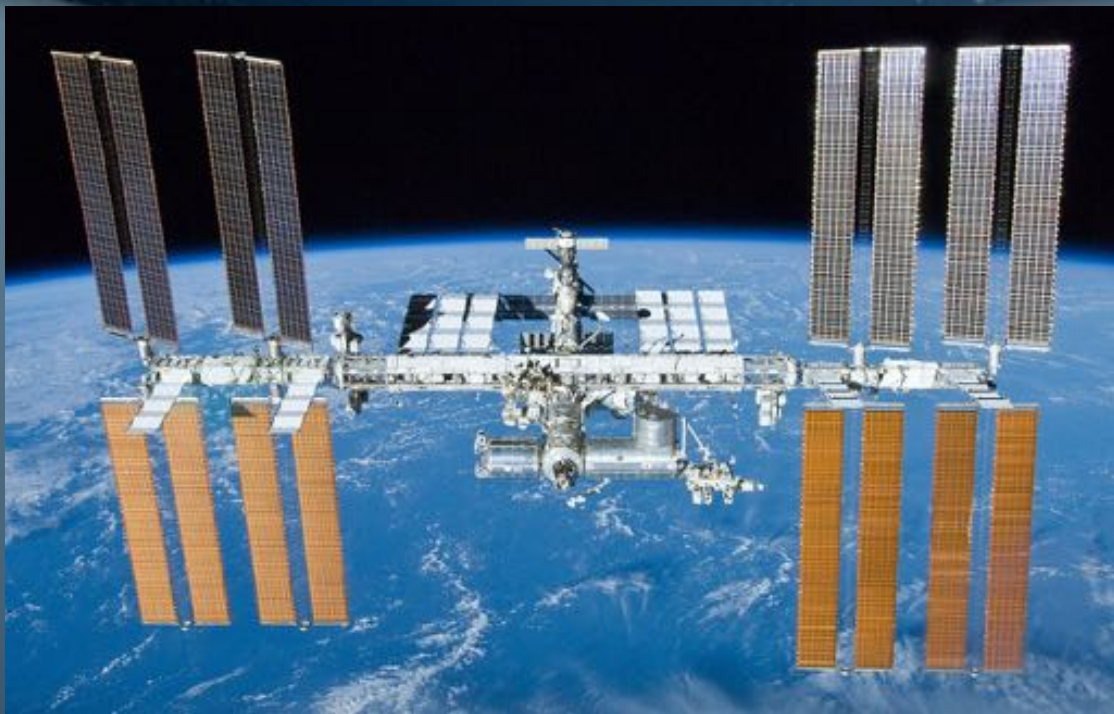


Pressure (Torr)	Sample	Applied voltage	R(Ohms)
$7.60 \times 10^{-2}$	coated Z93	40	$1.30 \times 10^{+8}$
	original Z93	40	$5.10 \times 10^{+8}$
$7.00 \times 10^{-1}$	coated Z93	40	$1.60 \times 10^{+8}$
	original Z93	40	$8.00 \times 10^{+10}$
$7.00 \times 10^{-2}$	coated Z93	40	$1.80 \times 10^{+8}$
	original Z93	40	$1.80 \times 10^{+11}$
$6.00 \times 10^{-2}$	coated Z93	100	$7.00 \times 10^{+7}$
	original Z93	100	$6.00 \times 10^{+10}$

As vacuum is increased the resistivity of the Z93 pigment powders increases several orders of magnitude while the indium oxide treated Z93P pigment remains relatively stable. This increase in resistivity can be attributed to either the removal of moisture within the bulk powder or the compression of the powder filling the void space allowing for an increased number of conduction paths.



# ISS Opportunity - MISSE-FF



The Materials ISS Experiment Flight Facility (MISSE-FF) with MISSE Sample Carriers (MSCs) in the fully open position exposing samples/experiments to the harsh environment of space in low-Earth Orbit (LEO). Image courtesy of Alpha Space.



An earlier MISSE mission



- Latest**
- Related**
- NASA TV Coverage Set for November Cygnus Launch to the International Space Station  
4 days ago
- Cygnus Dedicated to Astronaut John Young  
19 days ago
- Delings: The Little CubeSat That Could  
27 days ago
- NASA Launching Mars Lander Parachute Test from Wallops Sep. 7  
2 months ago
- Launch of Orbital ATK Antares From NASA's Wallops Flight Facility  
6 months ago
- NASA Sends New Research on Orbital ATK Mission to Space Station  
8 months ago



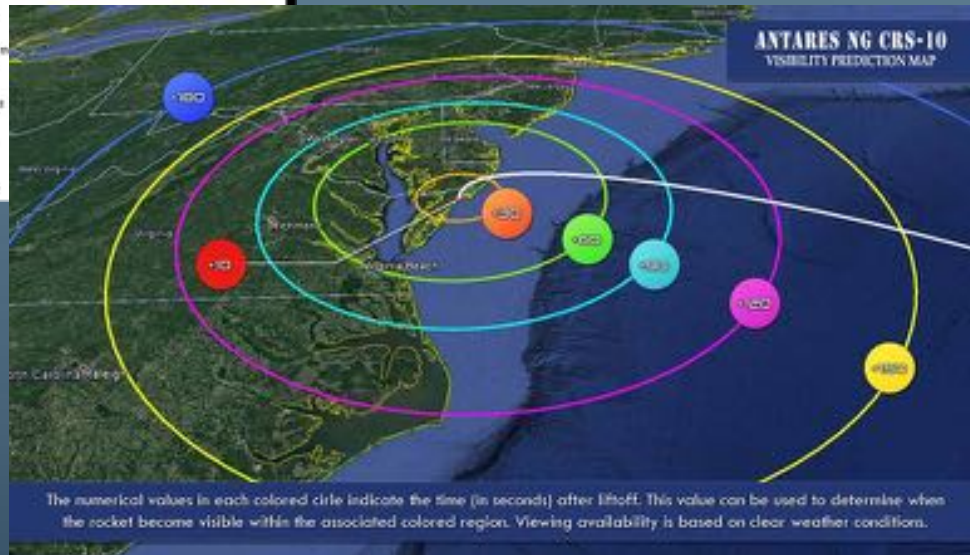
Nov. 8, 2018  
**Catch the Nov 17 Antares Launch from Wallops**

Get up early Nov. 15 to view the Northrop Grumman's Antares rocket launch from the Mid-Atlantic Regional Spaceport at NASA's Wallops Flight Facility.

The NASA Wallops Flight Facility and Virginia's Mid-Atlantic Regional Spaceport are set to support the launch of the Antares rocket, carrying the company's Cygnus cargo spacecraft to the International Space Station at 4:49 a.m. EST, Nov. 15.

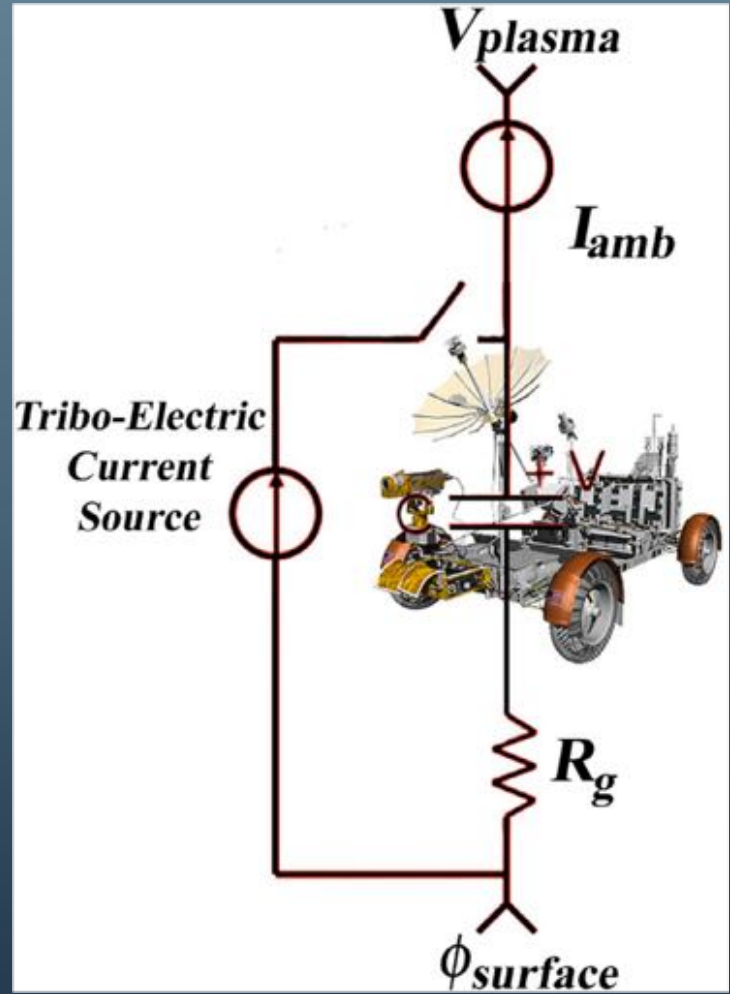
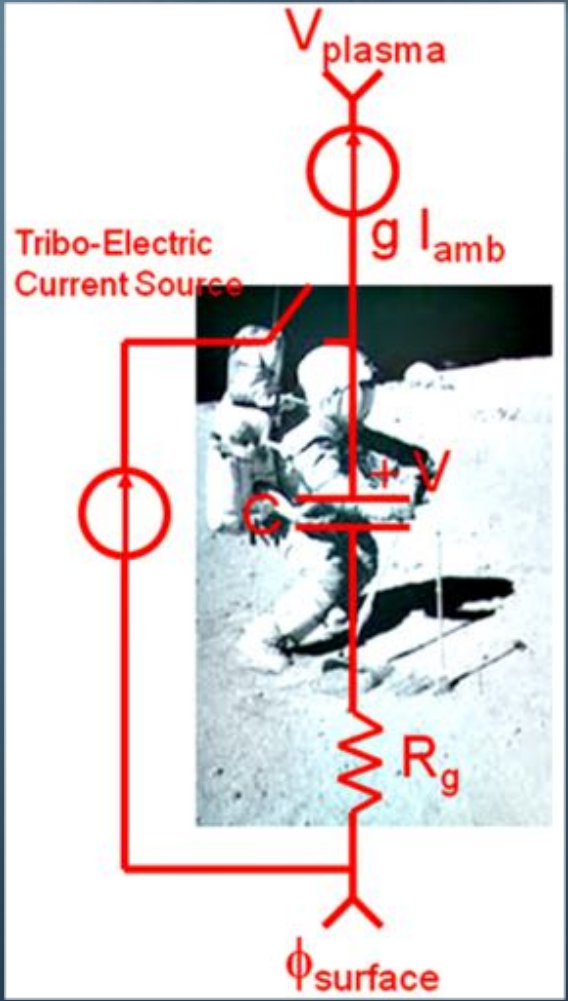
The launch may be visible, weather permitting, to residents throughout the East Coast of the United States.

The NASA Visitor Center at Wallops opens at 1 a.m. on launch day for public viewing. Additional locations for catching the launch are Robert Reed Park on Chincoteague Island or Beach Road spanning the area between Chincoteague and Assateague Islands. Assateague Island National Seashore/Chincoteague National Wildlife Refuge in Virginia will not be open for viewing the launch.





# Potential Applications



# CNT



## Problem

Observations of the Earth are extremely challenging; its large angular extent floods scientific instruments with high flux within and adjacent to the desired field of view

This bright light diffracts from instrument structures, rattles around and invariably contaminates measurements.

Astrophysical observations also are impacted by stray light that obscures very dim objects and degrades signal to noise in spectroscopic measurements.

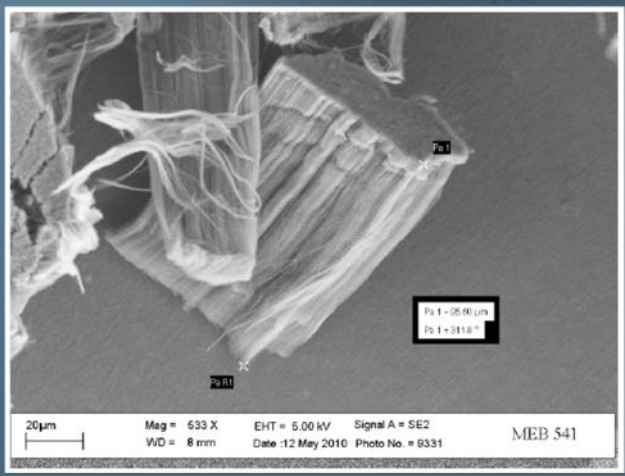
Stray light is controlled by utilizing low reflectance structural surface treatments and by using baffles and stops to limit this background noise

## Solution

In 2007 GSFC researchers discovered that Multiwalled Carbon Nanotubes (MWCNTs) are exceptionally good absorbers, with potential to provide order-of-magnitude improvement over current surface treatments and a resulting factor of 10,000 reduction in stray light when applied to an entire optical train.



# CNT



MWCNTs on silicon with alumina underlayer for enhanced adhesion

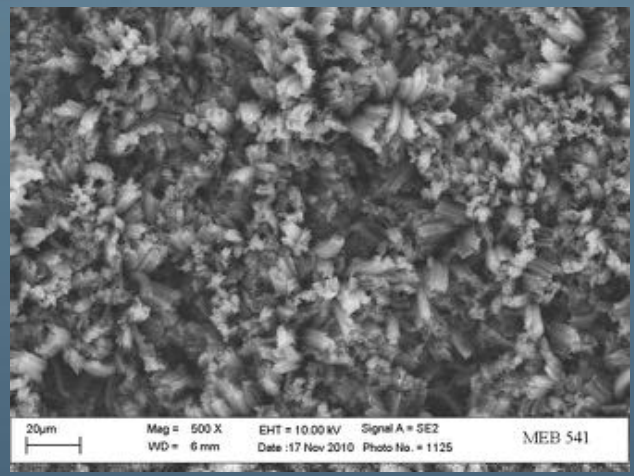


Image taken by electron microscope

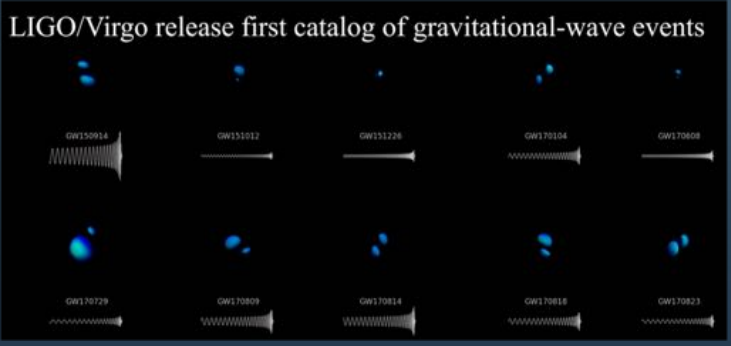
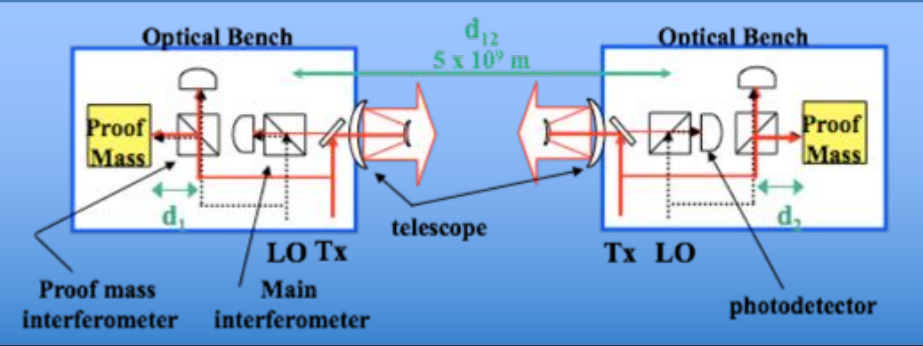
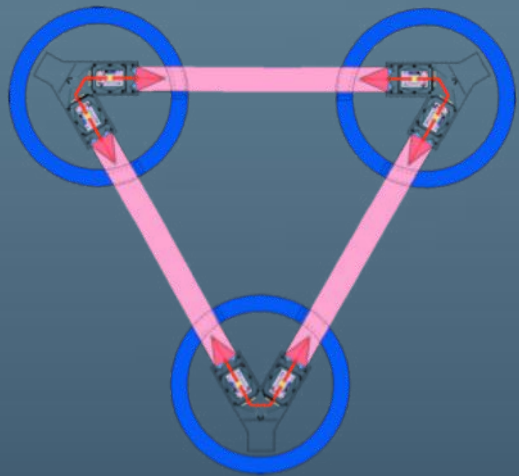
Tests indicate that the nanotube material is especially useful for a variety of spaceflight applications where observing in multiple wavelength bands is important to scientific discovery. The tiny gaps between the tubes collect and trap background light to prevent it from reflecting off surfaces and interfering with the light that scientists actually want to measure. Because only a small fraction of light reflects off the coating, the human eye and sensitive detectors see the material as black.



# Potential Applications

LIGO

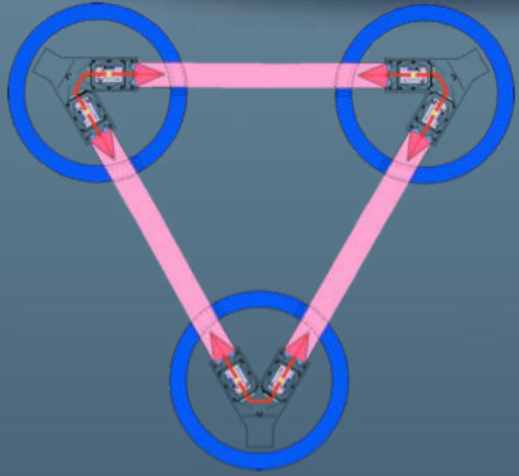
Laser Interferometer Space Array (LISA)





# Potential Applications

LIGO



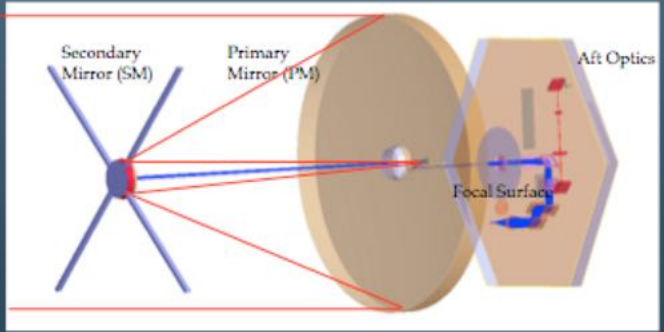
The transmitted laser beam is expanded to fill the telescope secondary mirror and then is reflected to the primary mirror to send a collimated beam between the sciencecraft.

The expanding transmitted beam fills the entire secondary mirror, simultaneous with the received beam, which is directed off of the primary mirror.

The received beam is however, obscured in the center of the secondary mirror by its own shadow.

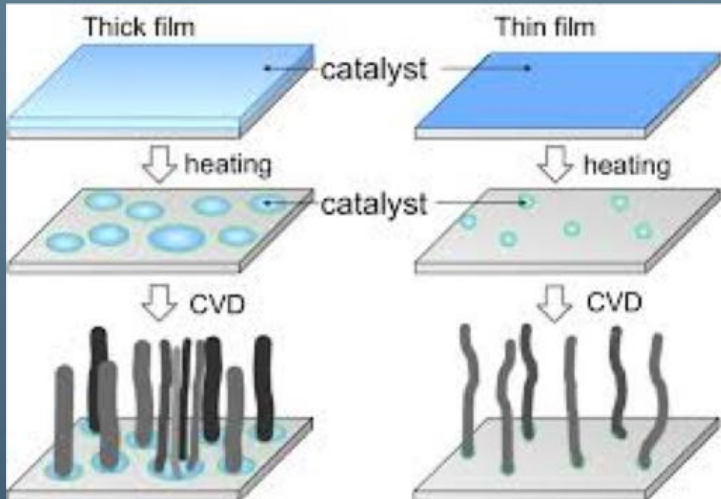
The issue is that the transmitted signal is nearly on axis to the center of the secondary mirror and will scatter light back to the focal surface and photodetector.

In this case the transmitted beam is 9 orders of magnitude higher in intensity and must be suppressed. This can be accomplished by blackening the center of the secondary mirror or by putting a hole in the center of the secondary mirror with an absorber in the back of it.

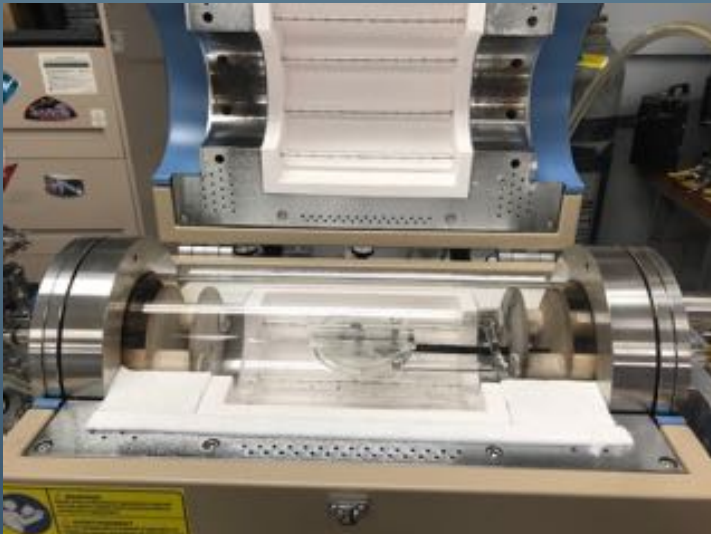


# Growth of CNT & ALD

## Typical Growth of CNTs



Substrate + Catalyst + Gas = CNNT  
 Si,Ti, flat, 3d + Iron,Ni + Ethylene

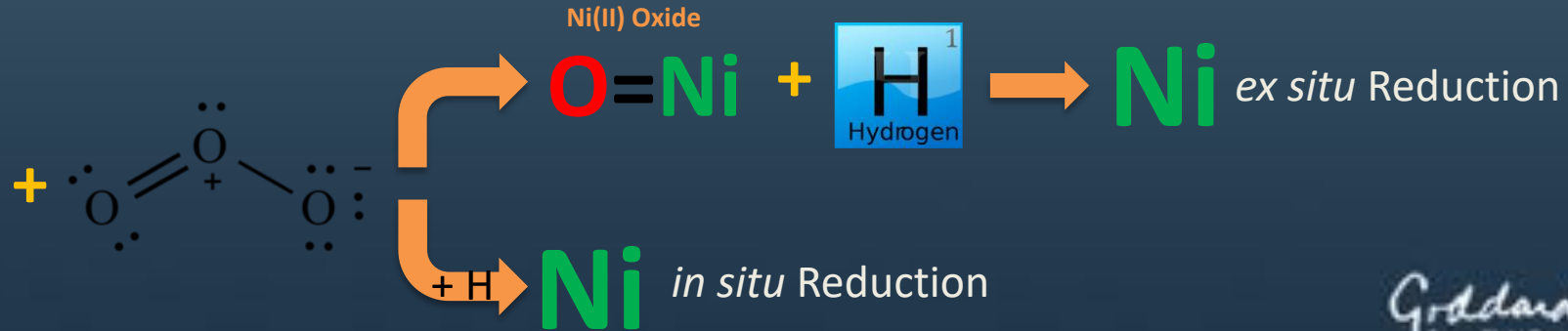
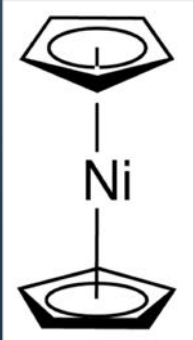


## ALD of Catalyst (Ni)

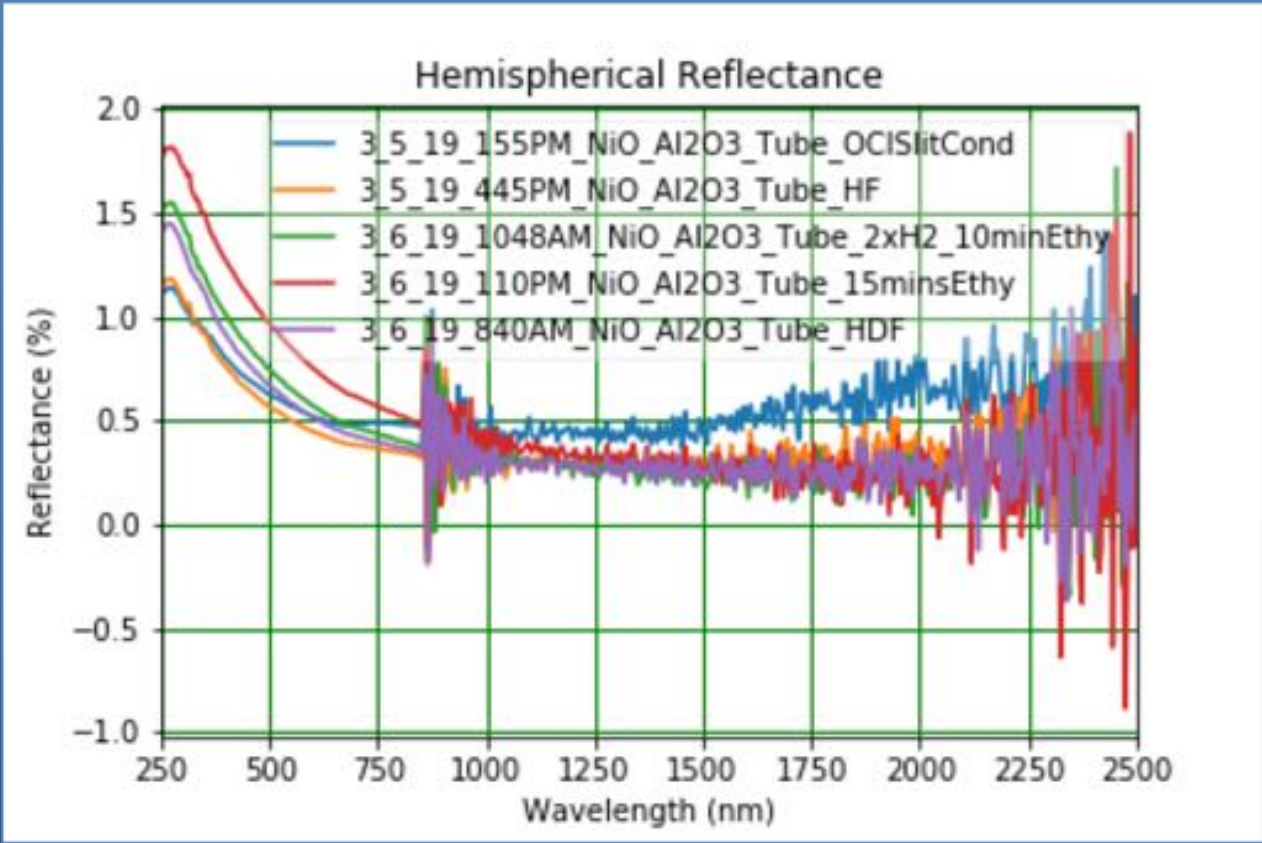
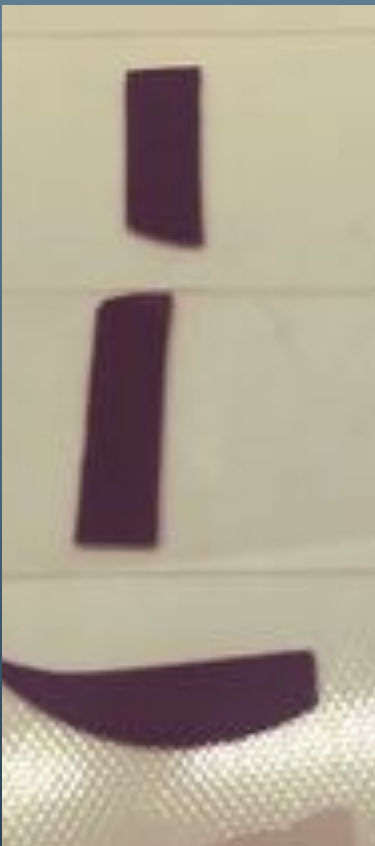
### Precursors and Reaction Pathway

Nickelocene

Ozone



# Initial Results





# Acknowledgments



Adomaitis Research Group



Mark Hasegawa

